STUDY OF FOULING AND MASS TRANSFER PROPERTIES OF CELLULOSE ACETATE-MODIFIED TFC MEMBRANES

ABURIDEH HANANE, ZIOUI DJAMILA, HOUT SARRA, BELGROUN ZOUBIR, YAHIAOUI FATMA ZOHRA and ABBAS MOHAMED

Unité de Développement des Equipements Solaires, UDES /Centre de Développement des Energies Renouvelables, CDER, Bou Ismail, 42415, W. Tipaza, Algeria
✉ *Corresponding author: H. Aburideh, h_aburideh@yahoo.fr*

Received June 11, 2024

The main objective of this work was to study the performance of thin-film composite (TFC) membranes developed for the treatment of saltwater. The synthesis of TFC polymer membranes was successfully achieved through interfacial polymerization between m-phenylenediamine (MPD) and trimesoyl chloride (TMC) on a 150 µm thick polyethersulfone (PES) support. The permeability and selectivity of the TFC membranes were investigated by incorporating cellulose acetate (CA) at various concentrations in an aqueous solution of MPD. The physicochemical properties of the prepared membranes were analyzed using FTIR, as well as in terms of water content and mass transfer characteristics. The optimized TFC membrane (TFC3; MPD: 2% by weight, CA: 5.7% by weight) exhibited improved efficiency in rejecting NaCl, $CaCO_3$, and $MgSO_4$, with respective rejection rates of 59.81%, 52.24%, and 62.53%, and a flux of 98 L/m².h. The flux recovery rate of this membrane was higher than that of the standard TFC membrane, indicating better resistance to fouling.

Keywords: cellulose acetate (CA), TFC membrane, fouling, flux, selectivity

INTRODUCTION

Water scarcity is a significant challenge that limits human growth and development. According to the United Nations World Water Development Report, approximately 780 million people currently lack access to safe drinking water, while the demand for process water is expected to increase by 400% globally between 2000 and 2050.[1] Desalination offers a promising solution for producing clean water from seawater. Desalination processes are generally categorized into thermal and membrane processes.[2] The thermal method typically involves energy-intensive multi-stage flash distillation (MSF) for treating high-salinity water,[3] whereas reverse osmosis (RO)-based membrane processes are less energy-intensive. RO is a well-established desalination technique that generates potable water from saline solutions.[4] Large-scale reverse osmosis plants are increasingly important due to the rising demand for pure water; for instance, the number of operating large-scale facilities has doubled over the past decade.[5] This technique continues to lead in the field of desalination, with numerous advancements made over the years in membrane materials, process modifications, module design, and pretreatment processes to enhance its efficiency and profitability.[6,7]

The membrane is the key element of the RO process. Its development began in the late 1950s when Loeb and Sourirajan invented the first practical membrane made of cellulose acetate.[6] This membrane dominated research and applications until the early 1980s, when John Cadotte developed the thin-film composite polyamide membrane through interfacial polymerization of m-phenylenediamine in an aqueous solution and trimesoyl chloride in an organic solvent.[7] The TFC membrane has since become the gold standard in RO processes, with ongoing efforts to enhance its performance through the incorporation of additives. Typically, the TFC membrane is a few hundred nanometers thick and is attached to a polymer backing sheet, such as polysulfone, manufactured using the phase inversion process.[2,8]

Desalination through membranes is explained by various theories, including the solution-diffusion theory, which describes how water and salt molecules diffuse within the polyamide layer and transport from one side to the other.[9] Additionally, strong hydrophilicity of the membrane is crucial, as it helps prevent biofouling and enhances water attraction.[10]

Much research in membrane technology has focused on developing new techniques and materials for membrane preparation to enhance overall performance. Structural modifications are necessary to ensure better permeability and selectivity, as well as good mechanical, chemical, and thermal resistance properties. To address these challenges, established methods for polymer membranes often involve introducing additional phases into the membrane matrix.

Interfacial polymerization (IP) is a technique used to create the active layers of organic composite films for reverse osmosis and nanofiltration (NF). This process involves condensation occurring at the interface on the surface of a porous support in the presence of two different monomers. IP is the most important technique for the commercial manufacturing of TFC membranes, as well as NF and RO membranes.[11]

A typical interfacial polymerization process involves an acyl chloride monomer dissolved in an organic phase and an amine monomer dissolved in an inorganic phase, which react at the interface between the two immiscible phases. Various amine monomers, such as piperazine (PIP) and MPD, along with acid chloride monomers like TMC and isophthaloyl chloride (IPC), have been utilized to enhance membrane performance.

Although the TFC-based reverse osmosis process is a mature technology, advances in these membranes – both in support and selective layers – continue to attract global research interest due to their significant application in desalination. Numerous contributions from scientists are reported each year aimed at improving TFC membrane performance and resolving operational issues. Nanoparticles (NPs), polymers, organic salts, and other additives have been incorporated to enhance the properties of TFC membranes.[12]

CA has played an important role in membrane technology, particularly in water and wastewater treatment applications. Activated hydroxyl groups in CA can be easily modified with other functional groups through reactions, such as oxidation, etherification, hydrolysis, esterification, grafting, cross-linking, and copolymerization.[13] CA exhibits better solubility in green solvents, and the availability of renewable resources makes it advantageous for many membrane applications, except in high-temperature settings. Furthermore, cellulose acetate, as an abundant polymeric material with a tunable chemical structure, is successfully employed in nanofiltration and reverse osmosis membranes due to several advantages: it is relatively inexpensive and readily available.[14] CA is a natural, biodegradable polymer that is environmentally safe, non-toxic, and offers significant design versatility.[15] One of the key advantages of CA is its low toxicity and biodegradability, along with its ability to enhance the effectiveness of TFC membranes. Additionally, it exhibits excellent chlorine resistance.

In recent decades, researchers have refocused on CA membranes for various applications, primarily due to environmental considerations. In the late 1950s, Reid and Breton (1959) demonstrated that CA membranes are highly impermeable to salts, but permeable to water.[16] Alongside their work on homogeneous CA membranes, Loeb and Sourirajan (1963) developed modified asymmetric CA membranes that maintained the same high salt rejection as homogeneous membranes, but achieved a much higher permeation rate.[17]

In other words, the advantageous surface properties and functional groups inherent to cellulose-based materials present significant opportunities for improving the overall performance of membranes. Cellulose-based materials, for instance, are typically highly hydrophilic due to the abundance of oxygen-containing functional groups on their surfaces. It has been demonstrated that increasing hydrophilicity not only enhances membrane permeability, but also imparts antifouling properties, particularly against organic pollutants, which remains a major challenge in water treatment.[18]

Furthermore, the hydrophilic charge can directly influence the diffusion of amine monomers in the organic phase, thereby significantly regulating the formation of the selective layer.[19-20] In addition, the plentiful functional groups on cellulose chains facilitate

further functionalization, which can be advantageous for introducing surface charge to the membrane, thus aiding in the removal of undesired contaminants.[21] Various functional groups/molecules, such as zwitterions, quaternary amines, carboxyl groups, phosphate groups, and ethylenediaminetetraacetic acid (EDTA), among others, have been successfully utilized for this purpose, as demonstrated in the literature.[22]

Therefore, by selecting the appropriate functional groups, functionalized cellulose particles can be specifically engineered to achieve the desired separation goals. Given that changes in performance and the enhancement of separation efficacy in TFC composite membranes are strongly influenced by the size and concentration of chemical functional groups, as well as the surface charge, cellulose-based nanomaterials with varied physical and chemical properties represent promising candidates for enhancing separation performance.

This work focuses on creating new membrane materials with enhanced performance and improved properties by incorporating hydrophilic molecules during the interfacial polymerization (IP) step of thin-film composite (TFC) polyamide membranes. The goal is to improve the balance between flux and selectivity of the membranes. The study aims to evaluate the effectiveness of these membranes by examining the influence of several parameters and validating their performance in terms of flux and rejection rate, while optimizing selectivity and extending their lifespan.

The purpose of this study is to explore the feasibility of combining the strengths of cellulosic derivatives in TFCs to design superior RO membranes for seawater desalination. The initial phase involves incorporating cellulose acetate into the inorganic MDP component of the TFC membrane at varying concentrations and subjecting the resulting membrane films to post-treatment. The second phase focuses on validating the membranes' performance in terms of rejection rate, while maintaining optimal flux, and studying the behavior of the membranes regarding clogging and desalination efficiency, in order to evaluate the potential of the hydrophilic cellulose derivative integrated into TFC membranes.

EXPERIMENTAL

Materials

Polyethersulfone (PES) [CAS: 25608-63-3; Chemical name: Poly(oxy-1,4-phenylenesulfonyl-1,4-phenylene)] was supplied by Sigma Aldrich (Germany). Cellulose acetate (CA) from Sigma Aldrich Chemistry (USA) [CAS: 9004-35-7; M = 50,000 g/mol] was used as a hydrophilic cellulose derivative. m-Phenylenediamine (MPD), obtained from BIOCHEM [CAS: 108-45-2; M = 108.14 g/mol], served as the diamine substrate for preparing the inorganic component. Trimesoyl chloride (TMC) [CAS No.: 31852-84-3; M = 108.14 g/mol; Chemical formula: $(C_4H_6O_3)n$], provided by VWR Chemical, was selected as the chloridic derivative for conducting the IP interfacial polymerization. Bovine serum albumin (BSA), characterized by a molecular weight of approximately 67 kDa, was purchased from Sigma and used to test adsorption on materials. Additional products tested for filtration experiments and analytical techniques include salts, such as sodium chloride (NaCl), calcium carbonate ($CaCO_3$), obtained from Biochem Lab, and magnesium sulfate ($MgSO_4$), purchased from Sigma Aldrich.

Manufacturing of membranes

The PES membranes were prepared using the NIPS (non-solvent induced phase separation) method. The casting solution was created by dissolving 18% PES in 82% N,N-Dimethylformamide (DMF). A heating stirrer was employed to homogenize the solution at 200 rpm for 24 hours. The resulting viscous solution was spread onto a glass plate, adjusting the thickness to 150 µm using a casting knife. The glass plate was then immersed in a coagulation bath, where the immersed solution transformed into a film as a phase change occurred from a liquid phase (transparent) to a solid phase (whitish). The membrane film was moved into a bath of demineralized water for 24 hours to accelerate the exchange between solvent and non-solvent. All membranes were stored overnight in distilled water (pure water as a non-solvent) at room temperature.[23]

Preparation of thin film composites (TFC)

The formation of a crosslinked polyamide layer on the membrane was accomplished through interfacial polymerization, as described in the literature.[24] After removing excess water, the substrate was immersed in an aqueous solution containing 2 wt% m-phenylenediamine (MPD) for 10 minutes. The membrane surface was carefully wiped with a paper towel, and a rubber roller was used to remove excess MPD. A solution of n-hexane containing 0.05–0.2 wt% trimesoyl chloride (TMC) was poured onto the membrane surface and allowed to react for a predefined time, followed by washing with n-hexane. The resulting membranes were quickly air-dried and then further cross-linked at 60 °C for 15 minutes before being cooled in ambient air.

Preparation of cellulose acetate solution (X)

TFC membranes were modified by incorporating cellulose acetate as a hydrophilic additive in the

aqueous phase rich in MPD. The films obtained, referred to as TFC-X, are listed in Table 1. The acetate-based solutions were prepared according to the procedure described by Araki *et al.*[25] Briefly, a specified quantity of cellulose acetate was added to a solution of hydrochloric acid (11.6 mL) at 80 °C and stirred for 25 minutes. The reaction was then stopped by plunging the solution into deionized water to halt hydrolysis. Excess acid was removed by repeated centrifugation cycles at 4000 rpm for 15 minutes. Finally, the aqueous suspension was left overnight to obtain a gel form.

Table 1
Formulation and preparation of membranes

Membrane symbols	Support composition		Thin layer			Observation
	PES	DMF	TMC	MPD	AC	
PES	18	82	/	/	/	Immersed in water, dried in ambient air
TFC	18	82	2%	0.2%	/	Dried in the oven for 15 min
TFC1	18	82	2%	0.2%	1%	Immersed in solution, dried in the oven for 15 min
TFC2	18	82	2%	0.2%	3%	Immersed in solution, dried in the oven for 15 min
TFC3	18	82	2%	0.2%	5.7%	Immersed in solution, dried in the oven for 15 min

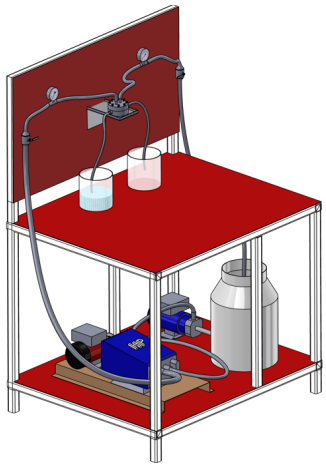

Figure 1: The filtration system unit

Characterization

The functional groups of the membrane films were examined using spectroscopy techniques. Attenuated total reflectance Fourier transform infrared (ATR-FTIR) spectroscopy (Frontier, Perkin Elmer) was utilized, with a range of 4000–500 cm^{-1} and a resolution of 0.5 cm^{-1}. The hydrophilicity of the TFC membrane surfaces was assessed by measuring the water absorption parameter to evaluate the hydrophilic/hydrophobic properties of the membranes. To determine the wet membrane weight, the membrane films were soaked in water for 24 hours, then dried with paper and weighed. They were subsequently dried in an oven at 80 °C for 24 hours, after which they were weighed again to determine the dry film weight.[26]

The water absorption rate was calculated from these two values using the following formula:

$$\text{Water absorption (\%)} = \frac{MW}{Md} x100 \quad (1)$$

where M_W: the weight of the wet membrane; M_d: the weight of the dry membrane.

Permeation test

The filtration system is illustrated in Figure 1. It consists of a filtration cell designed by Delta SRL (Rende (Cs), Italy) that accommodates flat membranes with a diameter of 60 mm, corresponding to a useful surface area of 28.4 cm^2. The membranes are always positioned on the active surface in contact with the feed solution. The pressure inside the cell is generated by a high-pressure pump. All measurements were conducted at transmembrane pressures ranging from 10 to 45 bars, with stirring in the feed tank to ensure solution homogeneity. For the filtration tests and evaluation of membrane performance, several compounds were used to study the selectivity of the membrane and assess its performance. These compounds include salts, such as NaCl (sodium chloride at 7 g/L), $MgSO_4$ (magnesium sulfate at 300 mg/L), and $CaCO_3$ (calcium carbonate at 300 mg/L).

The performance of the fabricated membranes was evaluated in a cross-flux filtration apparatus (RO

mode) by measuring the pure water flux (J) and the permeability coefficient (Lp) in $Lm^{-2}h^{-1}bar^{-1}$, along with NaCl rejection (R, %) at different pressures. These parameters were determined using the following equations:

$$J_w = \frac{\Delta V}{Am\Delta t} \quad (2)$$

$$Lp = \frac{J}{\Delta P} \quad (3)$$

where J is the pure water flux (L/m^2h^1), ΔV is the volume change of permeate water (L), Am is the membrane effective area (m^2), Δt is the testing time of filtration (h), and ΔP (bar) is the transmembrane pressure.

A feed NaCl solution was used for evaluation of the salt rejection (TR) and calculated using Equation (4). The feed and permeate concentrations were determined by conductivity measurement of the feed and permeate solutions and comparing them to a concentration-conductivity calibration curve.

$$TR = 1 - \frac{C_p}{C_A} \quad (4)$$

where C_A and Cp are the NaCl concentrations (M) in feed and permeate solutions, respectively.

Dynamic fouling experiment

The membrane fouling behavior was tested using bovine serum albumin (BSA) as a model,[27] with a molecular weight of approximately 67 kDa, at a concentration adjusted to 0.2 g/L. First, the pure water flux (JW) of the clean membrane was measured with deionized water at 20 bar for 30 min. Then, the flux of the solution (JP) of BSA crossing the membrane for 30 h was measured. The fouled membrane was washed with deionized water under static conditions for 15 min and the pure water flux (JR) of the washed membrane was remeasured.

The filtration and washing cycle was repeated 3 times. The flux recovery rates (FRR), total fouling (Rt), reversible fouling (Rr) and irreversible fouling (Rir) were calculated using Equations (5) to (8):

$$FRR(\%) = \frac{JR}{JW} \times 100 \quad (5)$$

$$Rt(\%) = (1 - \frac{JP}{JW}) \times 100 \quad (6)$$

$$\mathrm{Rr}\,(\%) = (\frac{JR - JP}{Jw}) \times 100 \quad (7)$$

$$\mathrm{Rir}\,(\%) = (\frac{Jw - JR}{Jw}) \times 100 \quad (8)$$

During all solute filtration experiments, the magnetic stirrer was used to provide vigorous mixing and reduce concentration polarization that might otherwise occur at the membrane surface. The experiments were carried out at room temperature.

RESULTS AND DISCUSSION

Chemical structure

To characterize the surface functional groups of the PES substrate and TFC membranes, FTIR analysis was performed, and the results are shown in Figure 2. The absorption peaks in the range of 1150–1250 cm^{-1}, observed in the spectra of all membranes studied, are attributed to the sulfone groups of the PES support. Specifically, the peaks between 1140 and 1152 cm^{-1} correspond to the symmetric stretching of the O=S=O bond.[28] A peak at 1240 cm^{-1} is associated with the asymmetric stretching of the C–O–C group and the stretching of the aromatic C=C bond in this sulfonated polymer. The characteristic peaks at 1578 and 1488 cm^{-1} are attributed to the stretching vibrations of the benzene ring and the C–C bond, respectively.[29]

In comparison with the PES membrane, additional peaks were observed in the TFC membranes within the 1640–1700 cm^{-1} region. Figure 3 shows a peak around 1660 cm^{-1}, which is attributed to the C=O stretching vibrations of the -CO-NH- groups, confirming the formation of amide groups via interfacial polymerization.[30] Another characteristic band of polyamide overlaps with that of PES, located around 1480 cm^{-1}, which is related to the O–H stretching vibrations of carboxylic groups that may have formed due to the hydrolysis of unreacted acyl chlorides from TMC. FTIR results suggest successful interfacial polymerization between MPD and TMC.[31]

Figure 4 presents the characteristic peaks of hydroxyl functional groups (O–H stretching) observed in the fabricated TFC membranes, with spectra ranging from 2976 to 3704 cm^{-1}.[32] These peaks are attributed to N–H and O–H stretching vibrations in MPD. The hydrophilic properties of the membrane can be enhanced due to the presence of organic groups, such as hydroxyl, carbonyl, and carboxylic groups in the TFC membrane.[32]

In conclusion, the FTIR results demonstrated the presence of various bands characteristic of the essential functional groups in the TFC membrane film. However, no bands indicative of intermolecular hydrogen bonding were detected. Overall, the developed membranes confirm the successful realization of TFC membrane films.

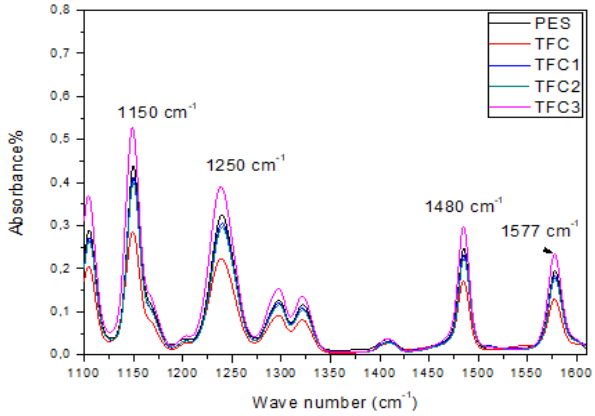

Figure 2: FTIR spectra of different membranes in the domain 1100-1600 cm^{-1}

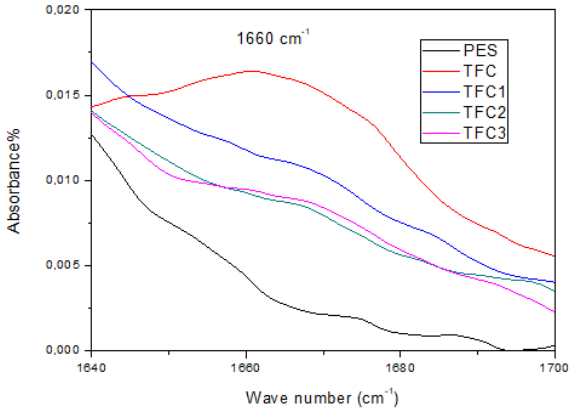

Figure 3: FTIR spectra of different membranes in the domain 1640-1700 cm^{-1}

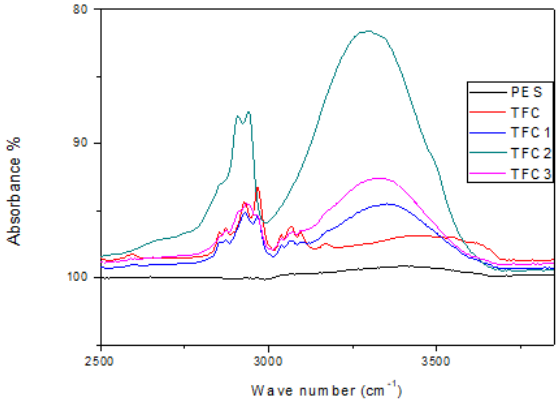

Figure 4: FTIR spectra of different membranes in the domain 2500-4000 cm^{-1}

Membrane performance

The plot of pure water permeation versus time, shown in Figure 5, indicates the different fluxes measured for the various membranes at a pressure of 15 bar. The flux of the PES membrane at this pressure is relatively low, approximately 28.82 L/m².h. In contrast, the flux decreases considerably for the pure TFC membrane (MDP/TMC), as this membrane is of the nanofiltration or reverse osmosis type, whereas the PES membrane is classified as an ultrafiltration (UF) membrane. The incorporation of cellulose acetate into the organic MDP solution led to an increase in flux. Specifically, the membrane with 1% cellulose acetate solution exhibited a flux of around 33.071 L/m²·h, while the flux reached 38.25 L/m².h for the membrane with 3% cellulose acetate, designated as TFC2. This indicates that introducing cellulose acetate at concentrations between 1% and 3% enhanced the hydrophilic properties of the membrane. However, when the cellulose acetate concentration was increased to 5.7% by weight, the flux showed a decrease similar to that of the pure TFC membrane, stabilizing around 20 L/m².h. This reduction can be attributed to the agglomeration of cellulose acetate on the membrane surface, which negatively impacts its performance in terms of flux.

Similar flux patterns were observed in Figures 6 and 7 for the different membranes at pressures of 25 and 45 bar. The flux remained constant throughout the operating time, demonstrating almost identical variation when transitioning to higher pressures. It is important to note that the optimum pressure corresponds to the maximum pressure applied, indicating an acceptable volumetric flux density ranging from 100 to 250 L/m²·h. This flux and pressure are suitable for the thresholds of nanofiltration and reverse osmosis membrane techniques, thus confirming the nanometric nature of the TFC membrane morphology.[33]

Figure 8 indicates that the permeability of the membranes is proportional to the flux, representing the inverse of the membrane's hydraulic resistance. The lowest permeability, equal to 3.06 L/m².h.bar, was observed for the

TFC3 membrane. In contrast, the TFC1 and TFC2 membranes exhibited the highest water permeability. This suggests that improving the hydrophilic nature of the membrane facilitates water diffusion through it. Several studies have concluded that membrane permeability is proportional to the number of pores, rather than the thickness of the membrane skin.[34-36] Moreover, only the skins of a membrane significantly impact its permeability. Thus, pore restriction leads to decreased permeability and increased membrane rejection, which explains the lower permeability value observed for the TFC3 membrane.

In conclusion, the incorporation of cellulose acetate into the TFC membrane enhances the rate of water penetration. The water flux of modified membranes is higher than that of unmodified membranes at cellulose acetate concentrations ranging from 1% to 3%. This supports previous research indicating that adding a hydrophilic polymer or additive improves hydraulic permeability and reduces hydraulic resistance. The water uptake behavior of the membrane is illustrated in Figure 9. This figure shows that the highest water content is observed for the TFC2 membrane, followed by the TFC1 membrane, with water contents of 51.39% and 47.83%, respectively. These membranes exhibit the best flux and permeability, confirming that increasing cellulose acetate levels from 1% to 3% leads to simultaneous increases in flux, permeability, and water absorption. Beyond this concentration, the distribution of cellulose molecules on the active layer affects its wettability and hydrophilic character.

Desalination performance

The graph in Figure 10 illustrates that the tested membranes effectively eliminate between 62% and 46% of divalent ions (Mg^{2+}, Ca^{2+}), achieving levels that meet the standards set by the WHO. However, their effectiveness in removing monovalent salts like NaCl is limited; for instance, the TFC3 membrane eliminates nearly 60% of this salt.

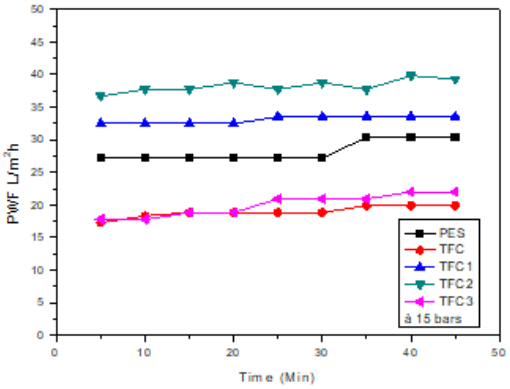

Figure 5: Evolution of pure water flux as a function of time (min) at 15 bar

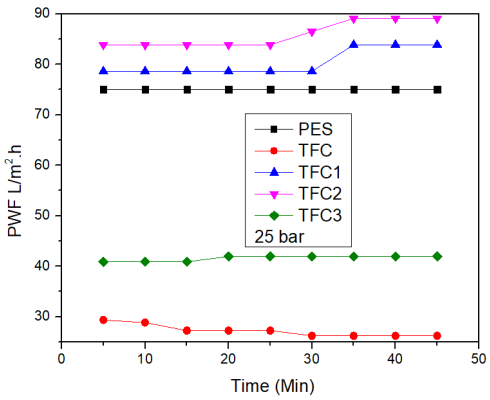

Figure 6: Evolution of pure water flux as a function of time (min) at 25 bar

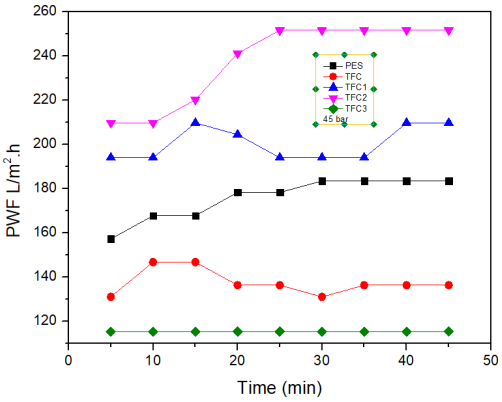

Figure 7: Evolution of pure water flux as a function of time (min) at 45 bar

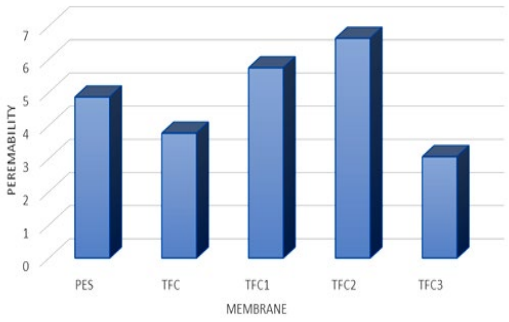

Figure 8: Hydraulic permeability of all membranes

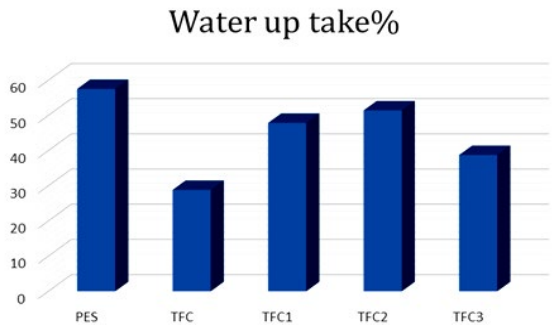

Figure 9: Water uptake parameter of all membranes

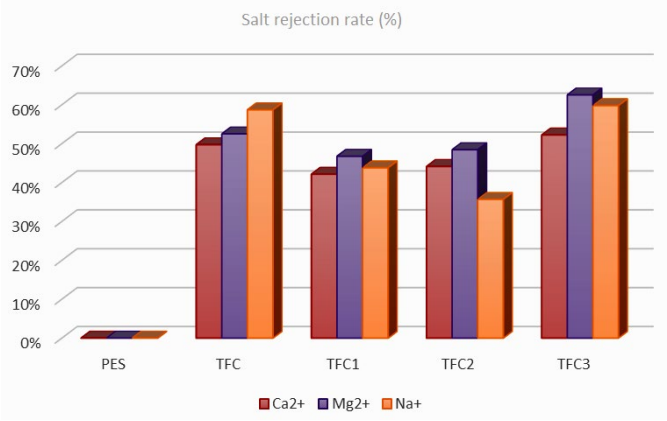

Figure 10: Rate rejection of di-monovalent salt for all membranes

The highest retention rates are observed in membranes characterized by lower filtration flux, specifically TFC3, followed by TFC. This inverse relationship between retention and flux supports previous findings. In conclusion, these membranes are useful for reducing water hardness and can contribute to the desalination of brackish water at low concentrations. These results indicate that the retention of monovalent salts is limited by the nanofiltration process.[37]

In summary, as illustrated in the graph, the study of salt elimination across different membranes revealed that the retention of di- and monovalent salts is highest for the TFC3 membrane, followed by the TFC membrane. However, this retention is still insufficient to meet the salinity standards set by the WHO. The salt rejection rates for the studied membranes follow this decreasing order: TFC3 > TFC > TFC2 > TFC1 > PES.

Consequently, the TFC3 membrane is deemed the most reliable and efficient for the removal of monovalent salts from a selectivity standpoint. It boasts optimal parameters with a flux rate of 57.64 L/m²·h·bar, and salt retention rates for NaCl, $CaCO_3$, and $MgSO_4$ are 59.81%, 52.24%, and 62.53%, respectively. These values affirm that this membrane exhibits properties consistent with nanofiltration membranes.

The pH readings obtained after treatment for each membrane are shown in Figure 11, displaying values between 6.9 and 7.5. These values comply with the standards required by the WHO and FAO, with acceptable limits between 6.5 and 8.2.[26] Regarding conductivity, there is a significant reduction from the initial value of 55.5 mS/cm, with the TFC3 membrane demonstrating a conductivity that is twice as low as the initial value. Other membranes have conductivities ranging between 45 and 52 mS/cm, confirming that they retain the least amount of undissolved solids.

TDS readings indicate a sharp decrease from a feed concentration of 36 g/L (which rises to 46 g/L when cycling the feed in a closed system). The TFC3 membrane shows the lowest TDS value at 14.17 g/L, followed by the TFC membrane, which indicates an elimination of 60.63% and 50.42%, respectively.

Antifouling property

Following the previous results regarding membrane performance, a significant reduction in flux was observed across the different solutions

studied. In this context, investigating membrane fouling phenomena is crucial. Fouling behavior was assessed using bovine serum albumin (BSA) as the fouling model at a concentration of 0.2 g/L for all membranes. Initially, the pure water flux (JW) of a clean membrane was measured using deionized water at 45 bar for 45 minutes. Subsequently, the BSA solution (denoted as JP) was tested on the membrane film for another 45 minutes. The filtration and washing cycle was repeated three times. Afterward, the fouled membrane was washed with deionized water to prepare it for reuse, and the pure water flux (JR) of the washed membrane was measured again.

Figure 11 illustrates the permeation flux of the BSA solution and pure water solutions at 45 bar as a function of time. The plot reveals a significant decrease in the flux of the BSA solution for all membranes. A similar reduction was noted during the second cycle of pure water filtration for all TFC membranes, indicating a considerable decline compared to the initial water flux. This decrease is primarily attributed to fouling by the BSA solution. Additionally, the fouling of the five membranes, along with concentration polarization, led to a rapid and sustained decrease in flux during the first 45 minutes, compared to that of pure water.

To further investigate the fouling phenomenon, additional coefficients were analyzed, including the recoveries for flux (TRF), total fouling (Rt), reversible fouling (Rr), and irreversible fouling (Rir), as shown in Figure 12. The results indicate that the TFC membranes demonstrate greater resistance to fouling compared to the PES membrane, which exhibits a flux recovery rate of 94%. The irreversibility rate for the PES membrane is the lowest at 18%, likely due to its ultrafiltration nature, which allows BSA molecules to pass through its pores, especially at high pressures.

Figure 11: Rejection rate of di-monovalent salt for all membranes

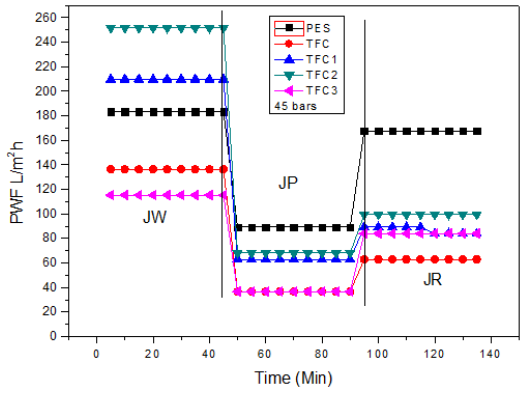

Figure 12: Time dependent pure water permeability (JW), BSA protein permeability (JP) and pure water permeability after washing with water (JR), for the neat membrane (PES) and TFC membranes

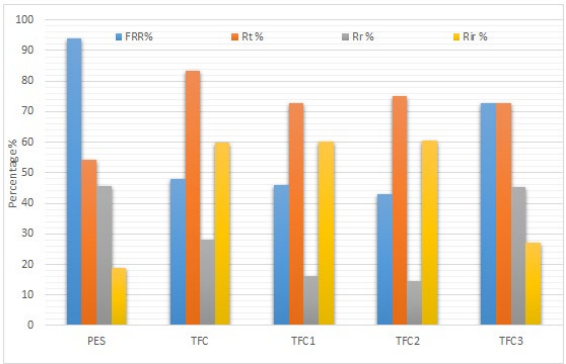

Figure 13: Flux recovery ratio (FRR), reversible fouling and irreversible fouling values for neat membrane (PES) and membranes TFC

In contrast, the TFC-x membranes display similar values for the different parameters (FRR, Rt, Rr, and Rir), with the exception of the TFC3 membrane. The reversible adsorption for membrane fouling caused by proteins is 45.5% for the TFC3 membrane, which is more

pronounced for the acetate-rich membrane. This can be explained by the deposition of material on the membrane's surface due to its lower permeability and narrower pore diameter. This clogging issue could potentially be mitigated by simple water washing or backwashing.

The TFC3 membrane, which is rich in cellulose acetate, exhibits the best TRF flux recovery rates and reversible TR clogging, attributable to the hydrophilic character imparted by the increased cellulose acetate content on the membrane's surface.[27] This hydrophilic property helps inhibit fouling adhesion and combats irreversible clogging. However, the relatively highest irreversible fouling (Rir) was observed for the TFC1 and TFC2 membranes, around 60%. This can be attributed to their high water absorption capacity, which enhances the adsorption of protein molecules on the membrane surface or facilitates the impaction of these molecules within the membranes.

CONCLUSION

TFC membranes were successfully fabricated using interfacial polymerization on a 150 µm thick polyester support, ensuring excellent mechanical strength and resistance to high-pressure compression. An ultra-thin polyamide active layer was formed through the condensation reaction between MPD and TMC on the surface of the porous support. To enhance the membranes' performance regarding flux and selectivity, a cellulose acetate solution was incorporated into the aqueous phase of the TFC membrane.

FTIR analysis confirmed the presence of characteristic functional group bands in the various components of the membranes. The wettability studies indicated that increasing the cellulose acetate concentration from 1% to 3% resulted in higher water absorption, which was accompanied by simultaneous increases in flux and permeability. However, at a higher concentration of 5.7%, the molecular weight of the cellulose acetate led to denser membrane pores, resulting in a more compact structure that negatively affected performance.

The performance of the developed membranes was evaluated in terms of flux and salt rejection. Notably, the TFC3 membrane achieved the highest NaCl retention rate, although this was still insufficient to meet salinity standards. In contrast, rejection rates for divalent salts (Mg^{2+} and Ca^{2+}) were satisfactory across all membranes, with TFC3 demonstrating optimal parameters: a flux of 57.64 L/m²·h at 45 bars, and retention rates of 62.53% for Mg^{2+} and 35% for Ca^{2+}, aligning with WHO standards.

Unlike the pure TFC membrane, which showed significant protein adsorption and organic fouling, the cellulose acetate-rich TFC3 membrane exhibited the best flux recovery rates (TRF) and reversible fouling characteristics. This improved performance is attributed to the enhanced hydrophilicity of the membrane surface due to the increased cellulose acetate content, which effectively mitigates fouling.

In summary, the incorporation of cellulose acetate into the TFC membranes significantly improves their performance and fouling resistance, making TFC3 the most reliable and efficient option for water treatment applications.

REFERENCES

[1] B. Hua, H. Xiong, M. Kadhom, L. Wang, G. Zhu *et al*., *Environ*. *Res*. *J*., **89**, 974 (2017), https://doi.org/10.2175/106143016x14696400494452

[2] H. Lonsdale, *J*. *Membr*. *Sci*., **10**, 81 (1982), https://doi.org/10.1016/s0376-7388(00)81408-8

[3] C. Fontàs, R. Tayeb, M. Dhahbi, E. Gaudichet, F. Thominette *et al*., *J*. *Membr*. *Sci*., **290**, 62 (2007), https://doi.org/10.1016/j.memsci.2006.12.019

[4] K. P. Lee, T. C. Arnot and D. Mattia, *J*. *Membr*. *Sci*., **370**, 1 (2011), https://doi.org/10.1016/j.memsci.2010 12.036

[5] D. Zioui, L. Aoudjit, Z. Tigrine, H. Aburideh and O. Arous, *J*. *Phys*. *Chem*. *A*, **96**, 1334 (2022), https://doi.org/10.1134/S0036024422060334

[6] P. Marchetti, M. F. Jimenez Solomon, G. Szekely and A. G. Livingston, *Chem*. *Rev*., **114**, 10735 (2014), https://doi.org/.10.1021/cr500006j

[7] A. Tsoukala, L. Peeva, A. G. Livingston and H. R. Bjorsvik, *ChemSusChem*, **9**, 188 (2012), https://doi.org/10. 1002/cssc.201100355

[8] H. Xiao, Y. Feng, W. R. F. Goundry and S. Karlsson, *Org*. *Process Res*. *Dev*., **22**, 891 (2024), https://doi.org/10.1021/acs.oprd.3c00470

[9] S. Karan, Z. Jiang and A. G. Livingston, *Science*, **348**, 1347 (2015), https://doi.org/10.1126/science.aaa5058

[10] H. Kim, S.-Y. Kwak, B.-H. Sohn and T. H. Park, *J*. *Membr*. *Sci*., **211**, 157 (2003), https://doi.org/10.1016/S0376-7388(02)00418-0

[11] P. P. Li, S. M. Xue, U. Shareef, Z. L. Xu and C. H. Ji, *J*. *Membr*. *Sci*., **624**, 119104 (2021), https://doi.org/10.1016/j.memsci.2021.119104

[12] M. Kadhom, *Chem*. *Eng*. *Res*. *Des*., **191**, 472 (2023), https://doi.org/10.1016/j.cherd.2023.02.002

[13] S. Tahazadeh, T. Mohammadi, M. A. Tofighy, S. Khanlari, H. Karimi *et al*., *J. Membr. Sci*., **638**, 119692 (2021), https://doi.org/10.1016/j.memsci.2021.119692
[14] S. Tahazadeh, H. Karimi, T. Mohammadi and M. Tofighy, *J. Solid State Chem*., **299**, 122180 (2021), https://doi.org/10.1016/j.jssc.2021.122180
[15] P. Zugenmaier, *Macromol. Symp*., **208**, 81 (2004), https://doi.org/10.1002/masy.200450407
[16] R. Candido, G. G. Godoy and A. R. Goncalves, *Carbohyd. Polym*., **167**, 280 (2017), https://doi.org/10.1016/j.carbpol.2017.03.057
[17] V. Vatanpour, M. Pasaoglu, H. Barzegar, O. Teber, R. Kaya *et al*., *Chemosphere*, **295**, 133914 (2022), https://doi.org/10.1016/j.chemosphere.2022.133914
[18] M. Shabin, A. Jamaliah and H. Raed, *Chemosphere*, **363**, 142927 (2024), https://doi.org/10.1016/j.chemosphere.2024.142927
[19] S. Mohammed, H. Hegab and R. Ou, *Chem. Eng. Res. Des*., **183**, 1 (2022), https://doi.org/10.1016/j.cherd.2022.04.039
[20] S. Mohammed, H. Hegab, R. Ou, S. Liu, H. Ma *et al*., *GreenChE*, **2,** 122 (2021), https://doi.org/10.1016/j.gce.2020.12.001
[21] H. Shaghaleh, X. Xu and S. Wang, *RSC Adv*., **8**, 825 (2018), https://doi.org/10.1039/c7ra11157f.
[22] Z. Wang, Z. Chen, Z. Zheng, H. Liu, L. Zhu *et al*., *Chem. Eng. J*., **451**, 138711 (2023), https://doi.org/10.1016/j.cej.2022.138711
[23] H. Aburideh, Z. Tigrine, L. Aoudjit, Z. Belgroun, K. Redjimi *et al*., *Cellulose Chem. Technol*., **55**, 1153 (2021), https://doi.org/10.35812/CelluloseChemTechnol.2021.55.99
[24] K. Guan, Y. Sasaki, Y. Jia, R. Gonzales and P. Zhang, *J. Membr. Sci*., **640**, 119801 (2021), https://doi.org/10.1016/j.memsci.2021.119801
[25] J. Araki, M. Wada, S. Kuga and T. Okano, *J. Wood Sci*., **45**, 258 (1999), https://doi.org/10.1007/BF01177736
[26] H. Aburideh, N. Kasbadji, M. W. Naceur, Z. Tigrine, D. Tassalit *et al*., *Cellulose Chem. Technol*., **53**, 583 (2019), https://doi.org/10.35812/CelluloseChemTechnol.2019.53.58
[27] H. Aburideh, Z. Tigrine, D. Zioui, S. Hout, D. Tassalit *et al*., *Cellulose Chem. Technol*., **55**, 697 (2021), https://doi.org/10.35812/CelluloseChemTechnol.2021.55.59
[28] M. A. Jafar, M. Mazumder, P. Raja, A. M. Isloor, M. Usman *et al*., *Sci. Rep*., **10**, 7049 (2020), https://doi.org/10.1038/s41598-020-63736-8
[29] Y. Chen, Y. Tao, J. Wang and S. Yang, *J. Polym. Sci*., *Part A*: *Polym. Chem*, **55**, 1313 (2017), https://doi.org/10.1002/pola.28496
[30] H. Bohra, S. Tan, J. Shao, C. Yang and A. Efrem, *Polym. Chem*., **7**, 6413 (2016), https://doi.org/10.1039/c6py01453d
[31] A.-H. Mostafa and A. El-Aassar, *Aust. J. Basic Appl. Sci*., **6**, 382 (2012)
[32] H. Aburideh, Z. Tigrine, D. Zioui, S. Hout, L. Aoudjit *et al*., *Cellulose Chem. Technol*., **57**, 911 (2023), https://doi.org/10.35812/CelluloseChemTechnol.2023.57.80
[33] J. Choi and M. Cho, *J. Chem. Phys*., **138**, 174108 (2013), https://doi.org/10.1063/1.4802991
[34] B. V. Bruggen, *J. Appl. Polym. Sci*., **114**, 630 (2009), https://doi.org/10.1002/app.30578
[35] K. A. Gebru and C. Das, *J. Environ. Manage*., **217**, 600 (2018), https://doi.org/10.1016/j.jenvman.2018.03.131
[36] V. Pereira, A. M. Isloor, U. K. Bhat, A. F. Ismail, A. Obaid *et al*., *RSC Adv*., **5**, 53874 (2015), https://doi:10.1039/C5RA07994B
[37] Z. Xu, J. Liao, H. Tang and L. Nanwen, *J. Membr. Sci*., **548**, 481 (2017), https://doi.org/10.1016/j.memsci.2017.11.064